Fatigue life prediction based on a mechanism-based simulation of crack initiation and short crack growth in forged Ti-6Al-4V

Hans-Jürgen Christ[1,*], **Helge Knobbe**[1], **Philipp Köster**[1,2], **Claus-Peter Fritzen**[2], **Martin Riedler**[3]

[1] Institut für Werkstofftechnik, Universität Siegen, D-57068 Siegen, Germany
[2] Institut für Mechanik und Regelungstechnik - Mechatronik, Universität Siegen, D-57068 Siegen, Germany
[3] Böhler Schmiedetechnik GmbH & Co KG, A-8605 Kapfenberg, Austria
* Corresponding author: Hans-Juergen.Christ@uni-siegen.de

Abstract Ti-6Al-4V was experimentally investigated in two different forged conditions with respect to fatigue crack initiation mechanisms and growth characteristics of microstructurally short fatigue cracks. The experimental findings show that the stage of short fatigue crack propagation is strongly affected by the microstructure and widely controls fatigue life under the testing conditions applied. The observations obtained were implemented into a mechanism-based short-crack model, which describes crack propagation as a partially irreversible dislocation glide on a crystallographic slip plane. The numerical model is based on dislocation dipole boundary elements. The non-uniform, oscillating propagation behaviour of short cracks is dealt with by defining grain boundaries and phase boundaries as obstacles to plastic slip and crack propagation. The model prediction in terms of short crack propagation behaviour allows for a quantitatively representation of the crack growth characteristics. Moreover, the simulation of short crack propagation was successfully used for the purpose of life assessment. Finally, by means of virtual microstructures, microstructural parameters such as grain size and volume fractions were systematically varied. Crack growth simulation calculations in these virtual microstructures are helpful to define those microstructural modifications which are desirable for improving the fatigue resistance.

Keywords Ti alloy Ti-6Al-4V, fatigue crack initiation, short fatigue crack propagation, microstructural barriers, fatigue life assessment, boundary element method

1. Introduction

The Ti6Al4V alloy is still by far the most common titanium material in use. It is used in many different fields, however the most important applications are probably found within the aerospace industry, where airframes and aero engine components are made of titanium alloys [1]. These employments are mainly driven by the superior structural efficiency of this alloy caused by an excellent combination of high strength and low density. Hence, a selection of high strength titanium forgings will always be found in the internal structure of planes.

A proper fatigue assessment is of course a crucial requirement for all structural components in flight service, since fatigue loading conditions always occur in these assemblies. Many approaches only consider the propagation of long cracks (damage tolerant approach) and thus make use of phenomenological equations such as Paris Law in classical linear elastic fracture mechanics [2]. As an alternative, total life approaches are used with S-N curves as basis for a fatigue life prediction according to Basquin/Coffin/Manson [3-5]. These methods do generally not distinguish between

crack initiation, short crack propagation and long crack propagation, which might be important in some cases. Another option, which is linked to physical properties of the material, is a microstructural-based short fatigue crack propagation model for lifetime prediction [6]. Since the loads arising in components associated with the internal structure are usually in the area of high cycle fatigue, up to 99% of the total lifetime can be spent with crack initiation and the propagation of short fatigue cracks. Thus, modeling short crack propagation in virtual microstructures promises a flexible and reliable approach for lifetime calculations. This paper presents firstly some selected experimental results from a study of the crack initiation and microstructurally short fatigue crack propagation mechanisms in two forged Ti6Al4V alloys. Then a mechanism-based model will briefly be introduced which tries to describe quantitatively the phenomena observed. This model will be verified by comparing experimental and predicted results. Finally it will be shown that by means of the generation of virtual microstructures the model is capable to identify microstructural parameters which are significant for a purposeful microstructure optimization with respect to fatigue resistance.

2. Material and experimental details

The Ti6Al4V alloy under investigation was delivered by Böhler Schmiedetechnik, where round bar stocks were forged into “V-shaped” pieces from which all specimens were machined. Two different heat treatments were applied after the forging process, (i) mill-annealing (ma) and (ii) solution heat treatment (sht). The most important chemical elements of the composition are given in Tab. 1. The analysis was done using spark emission spectroscopy. The figures represent mean values from three measurements and are within normal scatter. Some Fe content was found probably resulting from impurities of the alloying elements or from the process routine.

Table 1. Chemical composition in wt.%

Element	Al	V	Fe	Ti
Concentration	6.5	3.52	0.133	bal.

Micrographs using a scanning electron microscope with backscattered electron detector giving a channeling grain contrast of the resulting microstructures are shown in Fig. 1. A typical bi-modal microstructure was obtained in both conditions, thus no distinctive differences are present. The microstructures consist of primary alpha grains (α_p-grains) and colonies of secondary alpha lamellae (α_s-lamellae). A little content of remaining β-phase (app. 5-8%) can be found between the lamellae or at triple points.

The primary alpha grains of the sht microstructure are fully recrystallized due to the applied dwell time at a high temperature near the forging temperature, while the ma condition was cooled directly after forging, so some grains are only partially recrystallized. This can be deduced from orientation measurement data exhibiting large misorientation variations in single primary alpha grains along with subgrain boundaries.

The final heat treatment step was the same for both microstructures consisting of a plain stress relieve annealing above the Ti_3Al solvus temperature. The phase fractions are slightly different (α_p: 71% ma, 61% sht), and the mean grain sizes are larger for the sht condition (α_p: 3.1µm ma, 7.3µm sht; α_s: 3.3µm ma, 11.3µm sht). It should be mentioned that no subgrains were accounted for in the ma condition and that the α_s size refers to the colonies, meaning lamellae of the same orientation. Of course the mean lamella thickness is much smaller in case of the ma condition.

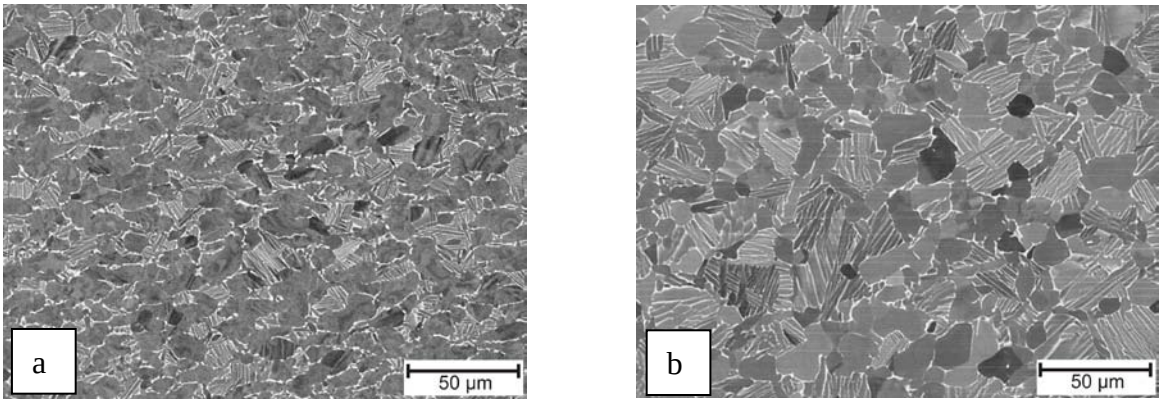

Figure 1. Microstructure of (a) ma condition and (b) sht condition.

All specimens except of the micro-sections were electro-chemically polished in a solution of perchloric acid and methanol prior to testing to meet the requirements for electron backscattered diffraction (EBSD) experiments. The surface should be as smooth as possible without any residual stresses from machining. This requirement can be perfectly met by grinding and vibration polishing (which was done in case of flat specimens for micro-sections), but is impossible for cylindrical specimens, where electrolytic polishing is the only possibility available. It should be pointed out that a slight surface roughness results from different metal removal rates of the different phases. The topography, measured by atomic force microscopy (AFM), was about 400nm from peak to valley.

Fatigue experiments were carried out in symmetrical push-pull with a servohydraulic MTS 810 test system under load control at a frequency of 20Hz. All experiments were stopped by specimen failure or at $6x10^6$ cycles. The samples which survived this number of cycles are referred to as run-out specimens. Cylindrical specimens with a milled shallow notch in the gauge length were used for the crack initiation and short crack growth investigations in order to limit the area to be observed. Some tests were interrupted after certain numbers of cycles to enable studying several cracks in the scanning electron microscope (SEM) together with EBSD. A Philips XL30 microscope equipped with automated orientation imaging microscopy (OIM^{TM}) was employed for all analytical research work. A FEI Helios DualBeam Microscope was used for sectioning cracks into the depth.

3. Experimental results

Two types of crack initiation sites were observed. Firstly, crack initiation is observed at the interface between two lamellae. Because of the Burgers relationship between alpha and beta phase

during phase transformation, this interface plane is parallel to one prismatic plane in the hcp crystal of the alpha phase, which is a possible slip system [7]. Secondly, cracks are found to initiate on slip bands inside of primary alpha grains.

Once initiated, different growth mechanisms were found for the short crack propagation in stage I. Inside of primary alpha grains or single lamellae, the crack grows on slip bands. By means of EBSD-measurements the cracks are identified to be either on the basal plane or the prismatic plane. The active slip bands are favorably orientated slip systems characterized by a high Schmid factor *S*. An example of such a crack is shown in Fig. 2a; the crack starts to grow on the basal plane with a Schmid factor of $S = 0.43$. After crossing a grain boundary the crack is slightly deflected and propagates on a prismatic plane, once again characterized by a high Schmid factor $S = 0.46$. Thus, the crack propagation rate is controlled by crack tip slide displacement range $\Delta CTSD$. The grain boundaries act as obstacles to crack propagation, as they prevent a transmission of slip into the neighboring grain. This yields a dislocation pile up in front of the barrier resulting in a decreased crack growth rate. If the boundary is overcome, the stress intensity will be relieved by slip in the next grain and the crack propagation rate will increase again, resulting in an oscillating crack growth rate. In addition to that, crack growth is also found on grain boundaries, as can be seen at the right crack tip in Fig. 2a. Here, the crack path is in a plane perpendicular to the applied load so that the normal stress, which causes a crack opening, seems to be responsible for crack propagation.

The crack in Fig. 2b grows on the interface between two lamellae. As this plane is equal to a prismatic plane with a Schmid factor of $S = 0.49$ the crack growth mechanism can be explained by slip as well. However, cracks were also found between two lamellae oriented normal to the applied load, where the Schmid factor on the respective prismatic plane is small.

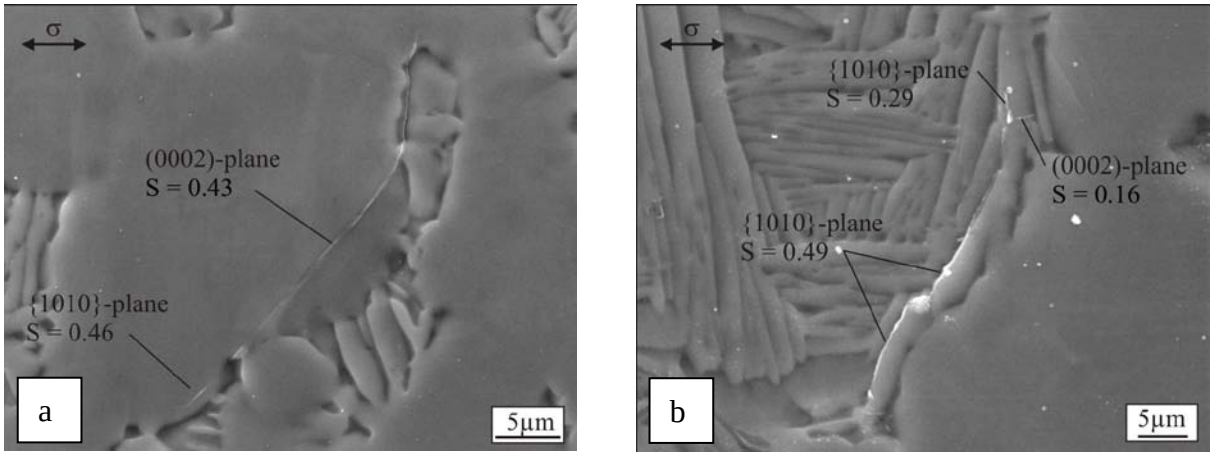

Figure 2. (a) Stage I-crack in primary alpha on slip plane and (b) crack growth on lamellae interface .

Since orientation data from the surface was used to calculate the possible slip plane, FIB sectioning was applied to determine the crack path direction into the interior (Fig. 3). A comparison between the calculated tilt angle of the slip plane with the surface and the crack path in the depth shows a good agreement. This strongly supports the assumption of crack growth occurring on a single slip system. However, as soon as a grain boundary is crossed (indicated by the white line) the crack is slightly deflected as can be observed on the surface as well.

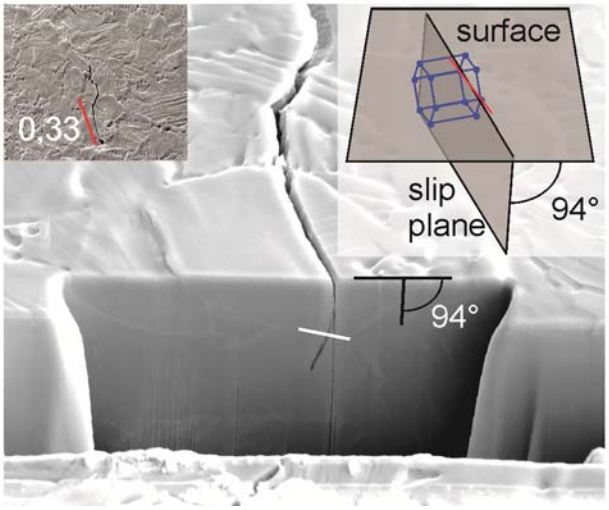

Figure 3. Cross section of a crack in primary alpha.

4. Short crack model

Several models for stage I-cracks have been presented, which consider the abnormal propagation behaviour of short cracks described above. Very promising one-dimensional analytical models for stage I-crack growth have been developed by Taira [8] and Navarro and de los Rios [9]. These models account for the barrier effect of grain and phase boundaries by blocking the extension of the plastic zone at the next grain boundary. Only if the stress on a dislocation source behind the grain boundary reaches a critical value, slip is transferred over the barrier resulting in an increased crack propagation rate. In order to take real microstructures with arbitrary grain shapes and orientations into account the analytical approaches have been extended to a two-dimensional model, which has been applied successfully to simulate crack growth in a duplex stainless steel [6,10]. This model is taken as the basis for the simulation of short crack growth in forged Ti6Al4V.

The crack problem is solved numerically by means of a discretisation with dislocation dipole boundary elements (see Fig. 4). Such a dipole element consists of a negative and a positive dislocation and represents a constant relative displacement over the element. Within a crack element two dipoles with a Burgers vector normal and tangential to the crack are combined to allow for an opening and a tangential displacement. On a slip band only a slide deformation is possible, so the respective boundary elements only consist of a dipole representing a tangential displacement. To monitor the stress state behind the grain boundary sensor elements with a constant length are positioned at the intersection point between active slip band and grain boundary. The sensor orientations match those of possible slip planes so that it is possible to calculate, in which direction a slip band is activated.

As grain boundaries act as obstacles to plastic deformation, the extension of the plastic zone is blocked by the next grain boundary. Thus, the crack propagation rate, which is controlled by the plastic deformation at the crack tip, decreases. Only if a critical stress intensity is reached on a dislocation source beyond the barrier in the neighbouring grain, the respective slip band is activated and the plastic zone extends into the new grain. The dislocation pile up in front of the grain

boundary is released resulting in a significant increase of the crack tip slide displacement and the crack propagation rate. This mechanism yields an oscillating crack growth rate that is characteristic of microstructurally short fatigue cracks.

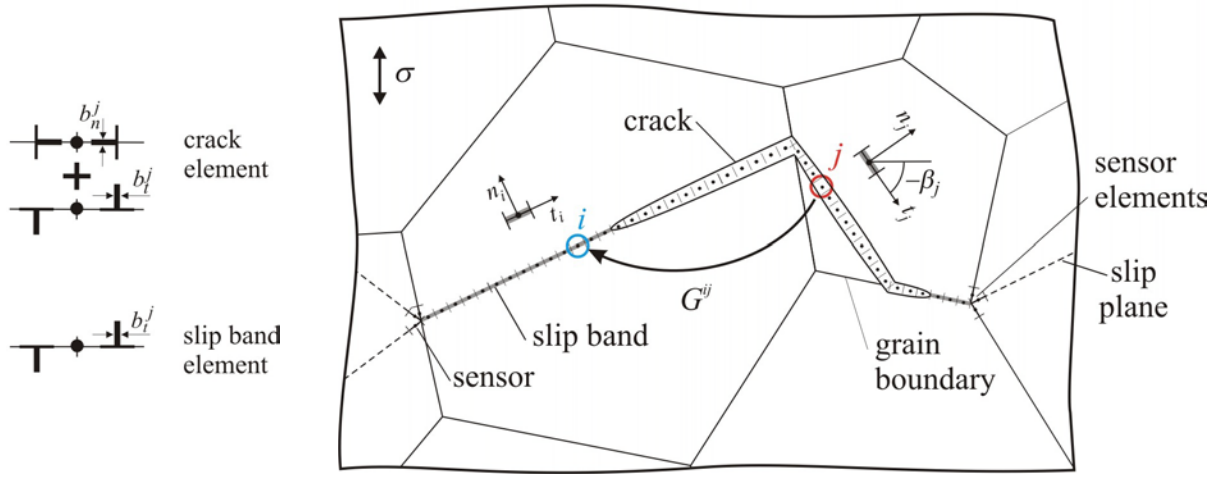

Figure 4. Stage I-crack model with boundary element discretisation.

In the plastic zone in front of the crack tip a differentiation between two cases is made, which results in different crack growth mechanisms. In the first case the crack propagates on a slip band and plastic slip occurs on this slip plane, if the resolved shear stress τ reaches the critical value for dislocation motion τ^b. In the second case the crack grows on a grain boundary, which does not represent a slip system of the crystal. Therefore, the only way to reduce the stress intensity in front of the crack tip is a plastic deformation inside the neighboring grains leading to a crack tip opening displacement. As the grains at each side of the grain boundary have different orientations, in general it is likely that more than one slip system is activated in each grain in order to ensure a compatible plastic deformation (Fig. 5a). In the model this plastic deformation is projected onto the yield strip on the grain boundary where both a tangential and a normal relative displacement is possible. As the plastic deformation occurs on multiple slip systems in the neighboring grains, the von Mises stress σ^m is used as the criterion for plastic deformation (Fig. 5b).

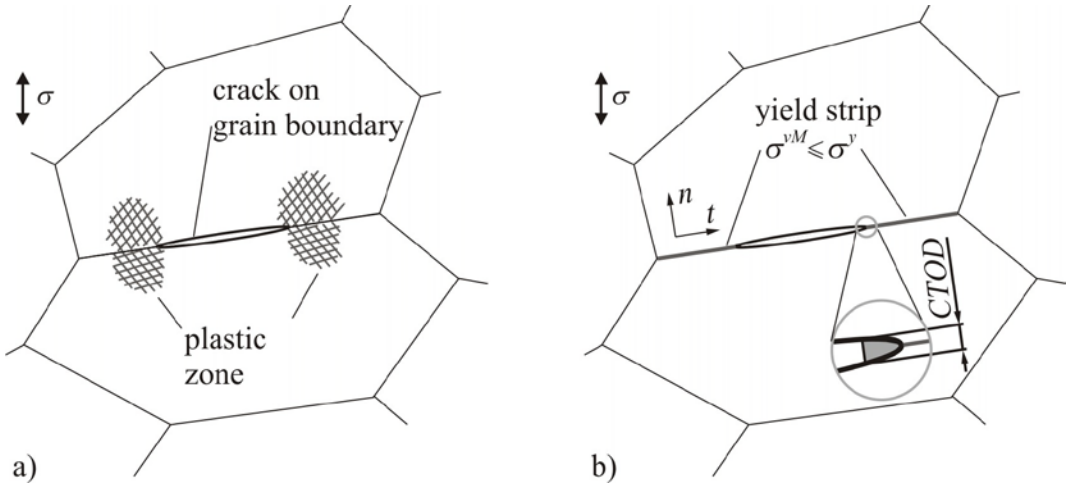

Figure. 5. Crack on grain boundary: a) plastic zone around the crack tip and b) yield strip model of the plastic zone.

The crack propagation on a slip band is calculated from the range of the crack tip slide displacement *ΔCTSD* by a power law function, which is analog to the model of [9]. A physical explanation for the mechanism of crack propagation is given in [11]. During the loading and the unloading cycle dislocations of opposite sign are created in a dislocation source in front of the crack tip and move towards the crack. Thus, vacancies are generated, which lead to a crack advance. For crack propagation on a grain boundary the crack growth is related to the range of the crack tip opening displacement *ΔCTOD*.

5. Virtual microstructure

The simulation model can be used for a virtual optimization of the microstructure for maximum high-cycle-fatigue strength. The aim is to carry out crack growth simulations in virtual microstructures with different properties to find out, how the stage I-crack growth resistance can be improved. Therefore, an algorithm for the generation of virtual microstructures has been developed, which is based on the Voronoi technique. Initially, such a Voronoi diagram has a normal distribution of the grain diameter and is single-phased. By assigning different phases to individual grains, a microstructure consisting of primary alpha grains and colonies of alpha lamellae is created. Furthermore, the average grain size and grain size distribution is modified by dividing selected grains.

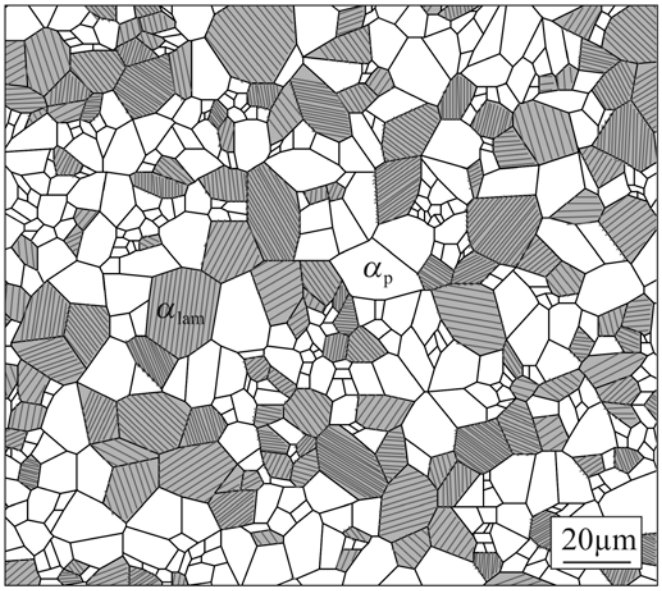

Figure 6. Virtual microstructure of forged Ti6Al4V in the sht condition.

In a first step a virtual microstructure has been generated, which represents the real microstructure of the ma condition shown in Fig. 1a. The virtual microstructure is shown in Fig. 6 and has a primary alpha volume fraction of 70.5%, compared to 70.9% of the real one. A good agreement is found in the mean diameter of the α_p-grains and lamellar grains, which are 10.0µm and 6.8µm for the virtual and 9.9µm and 6.8µm for the real microstructure. Also the grain size distribution shows a reasonably good agreement.

The slip systems in the model are chosen based on the experimental observations during the fatigue

tests. As cracks were found both on the basal plane and on prismatic planes in α_p-grains, the respective systems are considered in the model. In reality a lamellar colony consists of parallel alpha plates in a beta matrix and the orientation relation between both phases is defined by the Burgers relationship. This means that there are two parallel slip systems in both phases, and therefore slip can be easily transferred over the interface between alpha plate and beta matrix so that the effective slip length is equal to the colony diameter. As the effective slip length is the crucial parameter for crack initiation and crack growth, a lamellar colony is modeled as one grain in the virtual microstructure without resolving each single lamella.

6. Model capability

First, the model is verified by comparing simulation results to real fatigue crack propagation behavior. For this purpose the geometry of the crack shown in Fig. 7b is given as an input into the simulation model. Then, the simulation is started from the initial crack length until the crack tip reaches the end of the slip band. In Fig. 7a the projected crack length of the left and the right half is plotted over the number of cycles. It can be seen that the crack propagates fast on the left hand side on a slip band favorably oriented for slip. However, when the crack tip approaches the grain boundary the propagation rate decreases. On the right hand side the crack grows significantly slower on a grain boundary. The comparison of simulation and experimental data shows satisfying agreement.

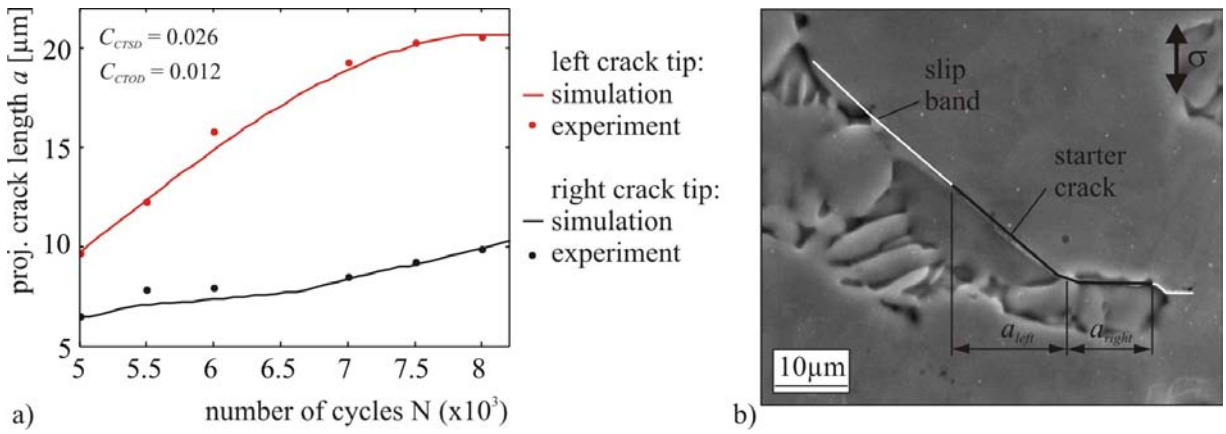

Figure 7. (a) Comparison between simulation and experimentally observed fatigue crack and (b) crack geometry.

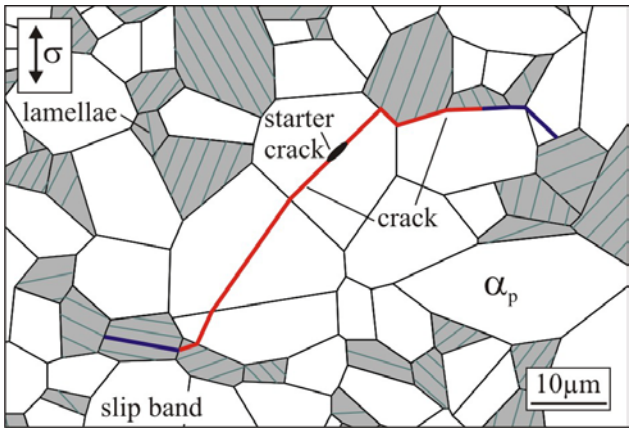

Figure 8. Crack growth simulation through several grains in virtual microstructure.

Crack growth simulations were carried out in virtual microstructures (Fig. 8). The simulation is started with an initial crack on a slip band in an α_p-grain. Then the crack grows autonomously through the microstructure. On the left hand side the crack propagates on a slip band, whereas intercrystalline crack growth on grain boundaries occurs on the right hand side.

On the basis of these calculations a fatigue life assessment is possible. For this purpose 100 calculations were carried out for each stress amplitude considered. A starter crack of 0.2µm in length is assumed to lie in the middle of an α_p grain, which is randomly selected from all α_p grains exhibiting a Schmid factor of higher than 0.4. In Fig. 9 the growth of the projected crack length with the number of cycles is shown for stress amplitudes of 500MPa and 600MPa. At the lower stress amplitude most of the cracks stop at microstructural obstacles.

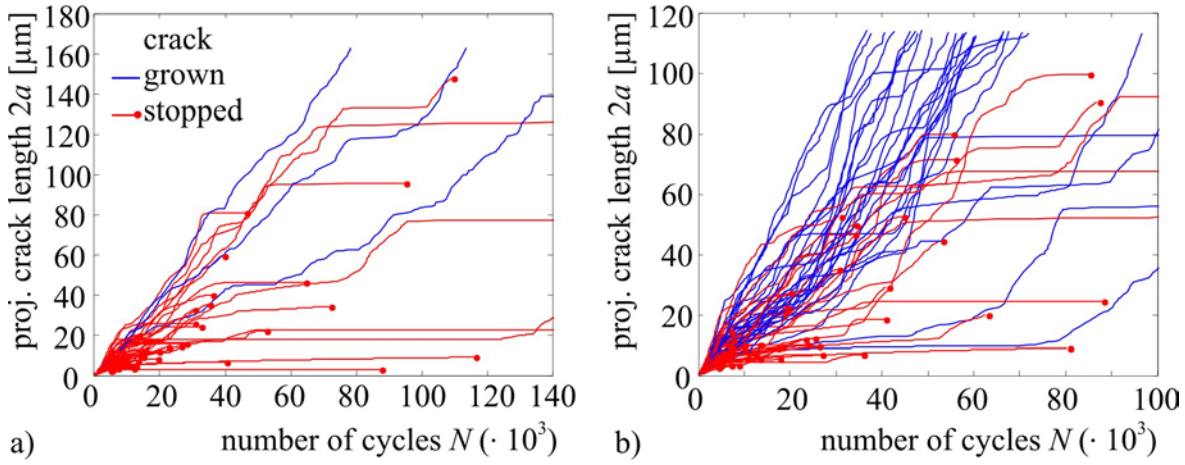

Figure 9. Crack growth simulation results for stress amplitudes of (a) 500MPa and (b) 600MPa (ma condition).

In these calculations, failure is defined to occur, when a critical value of the stress intensity factor at the crack tip is reached. This value is assumed to be 8 MPa $m^{½}$. In order to take into account that a real fatigue sample forms numerous fatigue cracks and that the fastest growing crack determines fatigue life, 20 cracks were randomly selected from the 100 cracks simulated and the one that fulfils the failure criterion first defines cyclic life. Hence 5 data points result for stress amplitude. This data is depicted in Fig. 10 together with the experimentally observed number of cycles until failure for both heat treatment conditions. The agreement appears very promising.

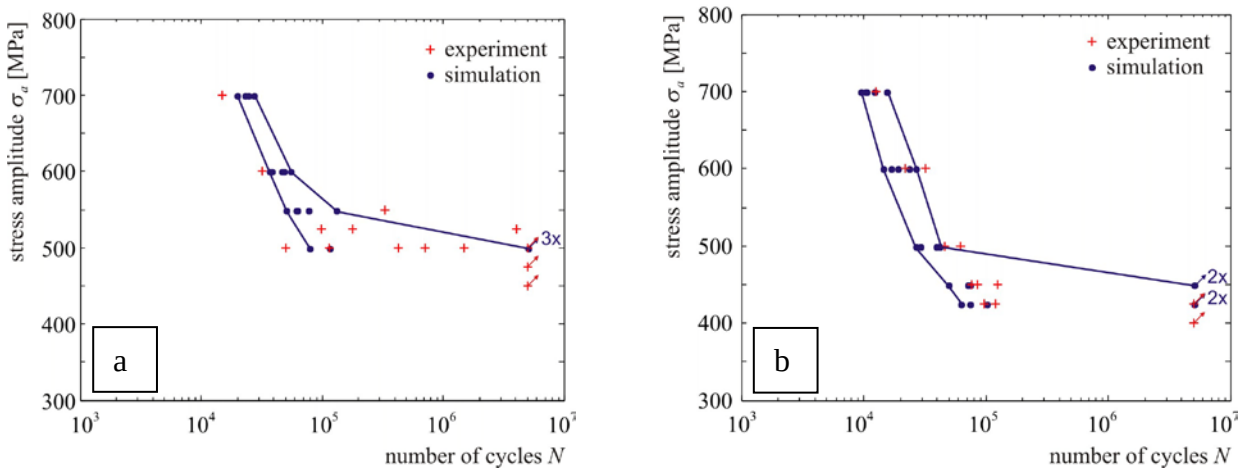

Figure 10. Comparison of observed and predicted fatigue lives for (a) ma condition and (b) sht condition.

7. Conclusions

This paper presents experimental investigations on crack initiation and short crack propagation in Ti6Al4V and shows, how the results are used in a numerical model. Crack growth mainly occurs on single slip systems (basal or prismatic) although in some cases cracks are found on boundaries where no slip system could be assigned. The numerical approach considers these crack growth mechanisms and uses either the range of the crack tip slide displacement or the crack tip opening displacement to describe the crack propagation rate. The modeling results show excellent agreement with propagation data of observed cracks. By means of calculations of the microstructurally controlled short fatigue crack growth in artificially generated "virtual" microstructures the significance and effect of microstructure parameters can be identified and analyzed, providing a mechanism-based foundation for a purposeful material development towards higher fatigue resistance. Moreover, a statistical treatment of the calculation results in terms of the evaluation of the distribution of the number of loading cycles necessary to reach a critical stress intensity factor under given loading conditions forms a sound methodology for fatigue life assessment.

Acknowledgement

The authors would like to express their gratitude to Böhler Schmiedetechnik GmbH & Co KG for financially supporting the project and supplying the material.

References:

[1] R.R. Boyer, An overview on the use of titanium in aerospace industry. Mat Sci Eng A, A213 (1996) 103-114.
[2] P.C. Paris, M.P. Gomez, W.E. Anderson, A rational analytic theory of fatigue. Trend Eng, 13 (1961) 9-14.
[3] O.H. Basquin, The exponential law of endurance tests. Proc Annual Meeting ASTM, 10 (1919) 625-634
[4] L.F. Coffin, Fatigue at high temperatures. ASTM STP, 520 (1973) 744-782.
[5] S.S. Manson, Fatigue: A complex subject-some simple approximations. J Exp Mech, 5 (1965) 193-226.
[6] B. Künkler, O. Düber, P. Köster, U. Krupp, C.P. Fritzen, H.-J. Christ, Modelling of short crack propagation – transition from stage I to stage II. Eng Frac Mech, 75 (2008) 715-725.
[7] G. Lütjering, J.C. Williams, Titanium (2nd Edition), Springe, Berlin-Heidelberg-New York, 2007.
[8] S. Taira, K. Tanaka, Y. Nakai, A model of crack-tip slip band blocked by grain boundary. Mechanics Research Communications, 5 (1978) 375-381.
[9] A. Navarro, E.R. de los Rios, Short and long fatigue crack growth: A unified model. Phil. Mag. A, 57 (1988) 15-36.
[10] O. Düber, B. Künkler, U. Krupp, H.-J. Christ, C.P. Fritzen, Experimental characterization and two-dimensional simulation of short-crack propagation in an austenitic–ferritic duplex steel. Int. J. of Fatigue, 28 (2006) 983-992.
[11] A.J. Wilkinson, S.G. Roberts, P.B. Hirsch, Modelling the threshold conditions for propagation of stage I fatigue cracks. Acta Mater, 46 (1998) 379-390.